

## DISCOVERY OF A WIDE BINARY BROWN DWARF BORN IN ISOLATION<sup>1</sup>

K. L. LUHMAN<sup>2,3</sup>, E. E. MAMAJEK<sup>4</sup>, P. R. ALLEN<sup>2</sup>, A. A. MUENCH<sup>5</sup>, AND D. P. FINKBEINER<sup>5</sup>

*Draft version November 14, 2018*

### ABSTRACT

During a survey for stars with disks in the Taurus star-forming region using the *Spitzer Space Telescope*, we have discovered a pair of young brown dwarfs, FU Tau A and B, in the Barnard 215 dark cloud. They have a projected angular separation of  $5.7''$ , corresponding to 800 AU at the distance of Taurus. To assess the nature of these two objects, we have obtained spectra of them and have constructed their spectral energy distributions. Both sources are young ( $\sim 1$  Myr) according to their H $\alpha$  emission, gravity-sensitive spectral features, and mid-IR excess emission. The proper motion of FU Tau A provides additional evidence of its membership in Taurus. We measure spectral types of M7.25 and M9.25 for FU Tau A and B, respectively, which correspond to masses of  $\sim 0.05$  and  $\sim 0.015 M_{\odot}$  according to the evolutionary models of Chabrier and Baraffe. FU Tau A is significantly overluminous relative to an isochrone passing through FU Tau B and relative to other members of Taurus near its spectral type, which may indicate that it is an unresolved binary. FU Tau A and B are likely to be components of a binary system based on the low probability ( $\sim 3 \times 10^{-4}$ ) that Taurus would produce two unrelated brown dwarfs with a projected separation of  $a \leq 6''$ . Barnard 215 contains only one other young star and is in a remote area of Taurus, making FU Tau A and B the first spectroscopically-confirmed brown dwarfs discovered forming in isolation rather than in a stellar cluster or aggregate. Because they were born in isolation and comprise a weakly bound binary, dynamical interactions with stars could not have played a role in their formation, and thus are not essential for the birth of brown dwarfs.

**ERRATUM:** The *K*-band magnitude for FU Tau B in Table 1 is incorrect and should be 13.33. The bolometric luminosity of FU Tau B in Table 3 and Figure 5 is incorrect because of that mistake and a separate arithmetic error. The correct value of the luminosity is  $0.0039 L_{\odot}$ . FU Tau A and B exhibited different isochronal ages in the original Hertzsprung-Russell diagram in Figure 5, which was unexpected for members of a binary system. This discrepancy is reduced in the corrected version of Figure 5 since both objects are now above the isochrone for 1 Myr. Given the large uncertainties in model isochrones at such young ages, the positions of FU Tau A and B in Figure 5 could be roughly consistent with coevality.

*Subject headings:* planetary systems: protoplanetary disks — stars: formation — stars: low-mass, brown dwarfs — binaries: visual — stars: pre-main sequence

### 1. INTRODUCTION

Several theoretical studies have suggested that dynamical interactions among young stars could be important – perhaps even essential – for the formation of brown dwarfs (Reipurth & Clarke 2001; Boss 2001; Bate et al. 2002; Delgado-Donate et al. 2003; Umbreit et al. 2005; Goodwin & Whitworth 2007; Stamatellos et al. 2007). In one of the proposed scenarios, the dynamical evolution of a group of protostars leads to the ejection of one of its members from the natal cloud core. Because its accretion is prematurely halted, the ejected object does not grow to

become a star. Alternatively, brown dwarfs might form through the fragmentation of circumstellar disks around protostars. The disruption of these binary systems by interactions with other stars in the surrounding cluster would then produce free-floating brown dwarfs.

According to early versions of the ejection models, binary brown dwarfs should have separations that are no larger than  $\sim 10$  AU (Bate et al. 2002). This prediction was consistent with the results from initial multiplicity surveys of brown dwarfs (Burgasser et al. 2007, references therein), but more recent observations have uncovered a small number of wide low-mass binaries in both the field and young clusters. Because of their fragile nature, it would seem difficult for a dynamical model to explain the existence of the widest and least massive systems ( $a \gtrsim 100$  AU,  $M_{tot} \lesssim 0.15 M_{\odot}$ ; White et al. 1999; Chauvin et al. 2004; Luhman 2004a; Billères et al. 2005; Allers 2006; Jayawardhana & Ivanov 2006; Caballero et al. 2006; Caballero 2007; Close et al. 2007; Artigau et al. 2007; Béjar et al. 2008). Nevertheless, in a new set of simulations, Bate et al. (2005) were able to produce a wide binary brown dwarf through the simultaneous ejection of two brown dwarfs in similar directions, indicating that the ejection models may remain

<sup>1</sup> Based on observations performed with the Magellan Telescopes at Las Campanas Observatory and the *Spitzer Space Telescope*.

<sup>2</sup> Department of Astronomy and Astrophysics, The Pennsylvania State University, University Park, PA 16802; kluhman@astro.psu.edu.

<sup>3</sup> Visiting Astronomer at the Infrared Telescope Facility, which is operated by the University of Hawaii under Cooperative Agreement no. NCC 5-538 with the National Aeronautics and Space Administration (NASA), Office of Space Science, Planetary Astronomy Program.

<sup>4</sup> Department of Physics and Astronomy, The University of Rochester, Rochester, NY 14627.

<sup>5</sup> Harvard-Smithsonian Center for Astrophysics, Cambridge, MA 02138.

viable. However, the feasibility of this formation mechanism for wide binaries depends on the environmental conditions of the star-forming cloud, particularly the stellar density. In fact, because the ejection models require the presence of a stellar cluster, brown dwarfs should not form in isolation, either as singles or binaries, if dynamical interactions are necessary for their formation.

The Taurus complex of molecular clouds is the most promising site in which one might find brown dwarfs that have been born in isolation. Taurus is the prototypical example of a low-density star forming region, is well-populated ( $\sim 400$  known members) and nearby ( $d = 140$  pc), and has been surveyed extensively for both stellar and substellar members (Kenyon et al. 2008). In this paper, we report the discovery of a wide binary brown dwarf in an isolated dark cloud in Taurus. We present optical and infrared (IR) photometry and spectroscopy for the components of the pair (§ 2) and use these data to measure their spectral types (§ 3.1), place them on the Hertzsprung-Russell (H-R) diagram (§ 3.2), and construct their spectral energy distributions (§ 3.3). We then assess the evidence that these two objects are members of Taurus (§ 3.4) and that they comprise a binary system (§ 3.5). Finally, we discuss the implications of this new binary system for the origin of brown dwarfs. (§ 4).

## 2. OBSERVATIONS

### 2.1. Background on FU Tau

The subject of this study is the star FU Tau, which is projected against the center of the Barnard 215 dark cloud (Barnard 1927)<sup>6</sup>. An optical image of FU Tau and Barnard 215 is shown in Figure 1. The cloud lies in a remote area of Taurus that is well-removed from most of the known members of the star-forming region, as illustrated by the map in Figure 2. FU Tau was first identified as a possible young star by Haro et al. (1953) through an H $\alpha$  objective prism survey (designated as Haro 6-7). As indicated by its name, FU Tau has exhibited significant variability (Kholopov et al. 1998), which is a common characteristic of young stars. Jones & Herbig (1979) identified it as a probable member of Taurus based on its proper motion. Despite the early evidence of the youth and membership of FU Tau, no other significant work has been done on it.

Luhman et al. (2006) used mid-IR images from the *Spitzer Space Telescope* (Werner et al. 2004) to search for new members of Taurus that have circumstellar disks. During a continuation of that survey, we identified FU Tau as a candidate based on its mid-IR excess emission. While performing optical spectroscopy on it, we noticed a fainter nearby object in the spectrometer's acquisition images. Because FU Tau is projected against the center of a dark cloud, an optically visible background star in close proximity to it was unexpected. Therefore, we elected to obtain a spectrum of this object to determine if it is a member of the cloud and a potential companion to FU Tau. The spectra confirmed that both FU Tau and the nearby source are young and have late spectral types. Hereafter in this paper, we refer to these objects as FU Tau A and FU Tau B. We describe

our spectroscopic observations of the pair in § 2.2. To obtain photometry and astrometry for FU Tau A and B, we have searched the public data archives of various observatories and wide-field surveys for optical and IR images that encompass their location. The data produced by this search are presented in § 2.3.

### 2.2. Spectroscopy

We obtained long-slit optical spectra of FU Tau A and B on the nights of 2007 December 17 and 18, respectively, using the Low Dispersion Survey Spectrograph (LDSS-3) on the Magellan II Telescope. The observations were performed with a 1.1'' slit, which was rotated to the parallactic angle. We used the VPH All and VPH Red grisms on the first and second nights, respectively, resulting in spectral resolutions of 10 and 5.5 Å at 7500 Å. We collected one 10 min exposure for the primary and three 20 min exposures for the secondary. After bias subtraction and flat-fielding, we extracted the spectra and wavelength calibrated them with arc lamp data. We then corrected the spectra for the sensitivity functions of the detectors, which were measured from observations of a spectrophotometric standard star.

FU Tau A was also observed at near-IR wavelengths using SpeX (Rayner et al. 2003) at the NASA Infrared Telescope Facility. On 2007 December 3, we operated SpeX in the prism mode with a 0.8'' slit, which produced a spectrum that extended from 0.8–2.5  $\mu\text{m}$  and that exhibited a resolving power of  $R = 100$ . On 2007 December 26, we collected another spectrum across the same wavelength range at higher resolution ( $R = 1000$ ) by using SpeX in the SXD mode with a 0.8'' slit. These data were reduced with the Spextool package (Cushing et al. 2004) and corrected for telluric absorption (Vacca et al. 2003).

### 2.3. Images

#### 2.3.1. 2MASS

Both components of FU Tau are detected in images at  $J$ ,  $H$ , and  $K_s$  from the Two-Micron All-Sky Survey (2MASS; Skrutskie et al. 2006). FU Tau A and B correspond to 2MASS J04233539+2503026 and J04233573+2502596, respectively, in the 2MASS Point Source Catalog. The 2MASS photometry of the primary should have negligible contamination from its companion given the large flux ratio of the pair at near-IR wavelengths ( $F_A/F_B \sim 40$ ). Those data are provided in Table 1. Because the secondary is only marginally resolved by 2MASS, the photometry reported in the Point Source Catalog may not be reliable. We do not use the 2MASS images for measuring the relative positions of FU Tau A and B since they are better resolved by data from other facilities.

#### 2.3.2. SDSS

Although it focused on areas of the sky at high galactic latitude, the Sloan Digital Sky Survey (SDSS; York et al. 2000) did obtain images of additional fields closer to the galactic plane (Finkbeiner et al. 2004). Those data encompassed a large portion of the Taurus cloud complex, including Barnard 215 (see Fig. 1). We have retrieved images and photometry of FU Tau in the five optical bands of SDSS (*ugriz*; Fukugita et al. 1996) from the Sixth Data Release of the survey (Adelman-McCarthy et al.

<sup>6</sup> Additional designations for this cloud include L1506E and L1506A (Lynds 1962; Nercessian et al. 1988; Lee & Myers 1999).

2008). The calibration of these images is described by Padmanabhan et al. (2008). Two sets of images are available for FU Tau, which were taken on 2002 December 6 and 31. The FWHM is  $\sim 1''$  for point sources in all bands at both epochs. The components of FU Tau are well-resolved from each other in these data. The primary was detected in each of the five bands while the secondary appeared in  $r$ ,  $i$ , and  $z$ . A variety of flux measurements are provided by the Sixth Data Release. For FU Tau A and B, we have selected the data measured with an aperture radius of  $1.745''$ , which is small enough to avoid contamination from the primary in the measurement of the secondary. Using other stars in these images, we measured aperture corrections for each band between radii of  $1.745''$  and  $7.43''$  and applied these corrections to the  $1.745''$  data for FU Tau A and B. For the photometric errors, we combine the Poisson errors in the source and background emission with uncertainties of  $\sim 5\%$  in the absolute calibrations. The SDSS photometry and relative astrometry for the components of FU Tau are listed in Tables 1 and 2, respectively.

### 2.3.3. CFHT

Guieu et al. (2006) obtained images at  $I$  and  $Z$  of the Barnard 215 cloud as a part of a wide-field survey of Taurus. These data were collected on the Canada-France-Hawaii Telescope (CFHT) with the CFH12K camera on 2002 December 29. The instrument contained twelve  $2048 \times 4096$  CCDs in a  $6 \times 2$  mosaic. The total field of view was  $42' \times 28'$ . We retrieved pipeline processed images of Barnard 215 and the associated photometric standards from the CFHT archive. One 30 s exposure and six 300 s exposures were available in each filter. The FWHM of stars in the  $I$ -band images is  $1\text{--}1.2''$ . One of the long  $I$ -band exposures of FU Tau is shown in Figure 3. We measured aperture photometry for the primary and secondary from the short and long  $I$ -band exposures, respectively. The photometry at  $I$  and relative astrometry are given in Tables 1 and 2, respectively. Because the photometric standards for these observations lack photometry at  $Z$  (Landolt 1992), we have not attempted to measure photometry from the images in this filter.

### 2.3.4. UKIDSS

The United Kingdom Infrared Telescope (UKIRT) Infrared Deep Sky Survey (UKIDSS, Lawrence et al. 2007)<sup>7</sup> is obtaining near-IR images of large areas of the northern sky. As a part of a survey of young nearby clusters, UKIDSS is in the process of imaging most of the Taurus star-forming region in  $Z$ ,  $Y$ ,  $J$ ,  $H$ , and  $K$ . The  $K$ -band observations of Barnard 215 were completed on 2005 December 31 and the resulting data products are now available to the public. We retrieved the  $K$ -band image and photometry for FU Tau from the first UKIDSS data release (Warren et al. 2007). Point sources in this image exhibit a FWHM of  $\sim 0.9''$ . The components of the binary are well-resolved, as shown in Figure 3. For a given object and band, UKIDSS provides several photo-

metric measurements that are based on a range of aperture radii. We present in Table 1 the  $K$ -band photometry for FU Tau B that was measured with an aperture radius of  $1''$  (Dye et al. 2006). UKIDSS photometry for the primary is unavailable since it is saturated. We measured the relative positions of the components of FU Tau from the UKIDSS image, which are given in Table 2.

### 2.3.5. Spitzer Space Telescope

As described in § 2.1, our study of FU Tau began during a survey for young stars with disks using mid-IR images of Taurus from the *Spitzer Space Telescope*. These images were obtained at 3.6, 4.5, 5.8, and  $8.0 \mu\text{m}$  with *Spitzer's* Infrared Array Camera (IRAC; Fazio et al. 2004). FU Tau appears within two sets of IRAC data. On 2005 February 23, the young star FT Tau, which is on the edge of Barnard 215 (see Fig. 1), was observed through the IRAC Guaranteed Time Observations of G. Fazio in *Spitzer* program 37. While the 3.6 and  $5.8 \mu\text{m}$  detectors were centered on FT Tau, the 4.5 and  $8.0 \mu\text{m}$  detectors observed an adjacent area of sky that happened to encompass FU Tau. The Astronomical Observation Request (AOR) identification for these data is 3964672. FU Tau also fell within a wide-field IRAC mosaic that was obtained through the *Spitzer* Legacy program of D. Padgett, which has a program identification of 30816. These observations were performed on 2007 March 30 and have AOR numbers of 19028480 and 19028224.

The IRAC images from 2005 and 2007 were processed with the *Spitzer* Science Center (SSC) S14.0.0 and S15.3.0 pipelines, respectively. The images produced by the pipelines were then combined using R. Gutermuth's WCSmosaic IDL package. The reduced images of FU Tau A and B at 3.6 and  $8.0 \mu\text{m}$  from the 2007 observations are shown in Figure 3. We measured aperture photometry for FU Tau A in the manner described by Luhman et al. (2008). We applied the same methods to the secondary except that we first removed light from the primary by subtracting a scaled IRAC point spread function (Marengo et al. 2006).

In addition to the IRAC data, images of FU Tau at  $24 \mu\text{m}$  have been obtained with the Multiband Imaging Photometer for *Spitzer* (MIPS; Rieke et al. 2004). These observations were performed on 2007 February 2 through D. Padgett's *Spitzer* Legacy program and have AOR numbers of 19026688 and 19027200. We measured aperture photometry for FU Tau A from the images produced by the SSC S16.1.0 pipeline (Luhman et al. 2008). FU Tau B is not resolved from the primary in these data.

The IRAC and MIPS measurements for FU Tau are presented in Table 1.

## 3. ANALYSIS

### 3.1. Spectral Classification

To investigate the properties of FU Tau A and B, we begin by using our optical and IR spectra to measure their spectral types and reddenings and to assess their ages. The optical spectra are shown in Figure 4. Both objects exhibit strong TiO and VO absorption bands, which are characteristic of late-M spectral types. The weak Na I, K I, and FeH absorption lines (Martín et al. 1996; Luhman et al. 1998; Gorlova et al. 2003; McGovern et al. 2004) and, in the case of the primary, triangular  $H$ -band continuum (Lucas et al. 2001)

<sup>7</sup> UKIDSS uses the UKIRT Wide Field Camera (WFCAM, Casali et al. 2007) and a photometric system described by Hewett et al. (2006). The pipeline processing and science archive are described by Irwin et al. (in preparation) and Hambly et al. (2008).

demonstrate that FU Tau A and B have the low surface gravities that are found in pre-main-sequence objects. The H $\alpha$  emission in each spectrum is also stronger than that found among field dwarfs (Gizis et al. 2002), providing additional evidence of youth. Thus, the spectra confirm that FU Tau A and B are young, low-mass objects.

We measured spectral types from the optical spectra by comparing them to averages of dwarfs and giants (Luhman 1999) and previously-classified members of Taurus and other star-forming regions (Briceño et al. 2002), arriving at M7.25 $\pm$ 0.25 and M9.25 $\pm$ 0.25 for the primary and secondary, respectively. To illustrate the derivation of these classifications, FU Tau A and B are compared to a selection of standards in Figure 4. FU Tau A matches closely with the average of a dwarf and a giant at M7.25 as well as the primary in the young binary 2MASS J11011926–7732383 (hereafter 2M 1101–7732, M7.25; Luhman 2004a). It is slightly cooler than the composite of the young eclipsing binary 2MASS J05352184–0546085 (hereafter 2M 0535–0546; Stassun et al. 2006), which has an optical spectral type of M6.75 (Luhman et al. 2007a). Meanwhile, FU Tau B is intermediate between an M9 dwarf/giant average and the Taurus member KPNO 4 (M9.5; Briceño et al. 2002). When we compare the IR spectrum of FU Tau A to previous SpeX data for optically-classified young objects (Muench et al. 2007), we derive an IR spectral type that is consistent with the optical measurement.

The slopes of the optical spectra of FU Tau A and B are similar to those of our bluest young standards, indicating they have low extinction ( $A_V < 1$ ). For instance, the optical spectrum of the primary has the same slope as Oph 1622–2405 A from Upper Sco (M7.25; Luhman et al. 2007a), which probably has little reddening since it is not associated with a molecular cloud. However, the 1–2.5  $\mu$ m spectrum of FU Tau A is redder than that of Oph 1622–2405 A by an amount that is equivalent to  $A_V = 2$  (Rieke & Lebofsky 1985). The same is true when we compare FU Tau A to other young M7 objects that appear to have negligible extinction, such as MHO 4, KPNO 2, and KPNO 5. This anomalous difference between the optical and IR reddening estimates for FU Tau A is probably not caused by errors in the spectra because the 0.6–1  $\mu$ m slopes of the LDSS-3, low-resolution SpeX data, and medium-resolution SpeX data are in good agreement while the 1–2.5  $\mu$ m slopes are the same among the two sets of SpeX data and the colors from 2MASS. It is possible that the IR spectrum appears too red because it is contaminated by long-wavelength emission from circumstellar dust, or the optical spectrum appears too blue because it is contaminated by scattered light or UV emission from accretion. To test the first hypothesis, we have compared the  $R = 1000$  K-band spectrum of FU Tau A to SpeX data for field dwarfs near the same spectral type (Cushing et al. 2004). We find no evidence for significant continuum emission from dust, which would cause the lines to appear weaker, or “veiled”, relative to those of a normal stellar photosphere. Thus, the slope of the IR spectrum of FU Tau A should accurately reflect its extinction. The alternative explanation is supported by the analysis of the spectral energy distribution (SED) of FU Tau A in § 3.3, which demonstrates the presence of short-wavelength ex-

cess emission.

### 3.2. H-R Diagram

To examine the masses and ages of the components of FU Tau, we can compare their effective temperatures and bolometric luminosities to the values predicted by theoretical evolutionary models. We have converted the spectral types of FU Tau A and B to effective temperatures with the temperature scale from Luhman et al. (2003). To estimate the luminosity of the primary, we have combined its  $J$ -band magnitude with the average bolometric correction for dwarfs near its spectral type (Dahn et al. 2002), an extinction of  $A_V = 2$  (§ 3.1), and a distance of 140 pc (Wichmann et al. 1998). For the secondary, we use its  $K$ -band magnitude since a reliable  $J$  measurement is not available. By doing so, we are assuming that any circumstellar disk that might reside around FU Tau B produces negligible emission at  $K$  compared to the stellar photosphere. This assumption is likely to be valid since disks around brown dwarfs rarely exhibit significant  $K$ -band excess emission (Luhman et al. 2008). The resulting temperatures and luminosities are listed in Table 3. The uncertainties in  $A_V$ , near-IR magnitudes, and bolometric corrections ( $\sigma \sim 0.14, 0.02, 0.1$ ) correspond to errors of  $\pm 0.07$  in the relative values of  $\log L_{\text{bol}}$ . When an uncertainty in the distance modulus is included ( $\sigma \sim 0.2$ ), the total uncertainties are  $\pm 0.11$ . These uncertainties do not include variability, which is known to be significant for the primary (Table 1; Kholopov et al. 1998).

Our temperature and luminosity estimates for FU Tau A and B are plotted on the H-R diagram in Figure 5 with the evolutionary models from Baraffe et al. (1998) and Chabrier et al. (2000). Although the components of binary systems are expected to be coeval, FU Tau A and B do not appear near the same model isochrone. The models imply an age of 1 Myr for the secondary while the primary is overluminous by an order of magnitude relative to that isochrone. The discrepancy is reduced somewhat if FU Tau A and B are compared to a fit to the cluster sequence for Chamaeleon I (Luhman 2007), which acts as an empirical isochrone. As shown in Figure 5, the primary and secondary appear 1.3 and 0.6 dex above this fit, respectively, resulting in a luminosity ratio that is 0.7 dex larger than expected for a coeval pair. FU Tau A is much brighter than other members of Taurus with similar spectral types whereas FU Tau B falls within the cluster sequence (Luhman 2004b), indicating that the difference in isochronal ages for the pair is a reflection of an anomalously high luminosity for the primary rather than a low luminosity for the secondary. One possible explanation is that FU Tau A is an unresolved binary. If so, it would appear near the upper envelope of the cluster sequence for Taurus in the H-R diagram, although it would remain overluminous relative to FU Tau B by  $\sim 0.4$  dex.

The data and models in Figure 5 imply a mass of  $\sim 0.015 M_{\odot}$  for FU Tau B. The model predictions do not encompass the temperature and luminosity of FU Tau A, and thus do not provide a direct estimate of its mass. However, because of the vertical nature of the mass tracks of low-mass stars and brown dwarfs at young ages ( $\tau < 10$  Myr), the spectral type of FU Tau A should provide a good indication of its mass regardless of lu-

minosity. As shown in Figure 5, the spectral type of FU Tau A combined with the adopted temperature scale and models imply a mass of  $\sim 0.05 M_{\odot}$ . This estimate is consistent with the fact that FU Tau A is slightly cooler than 2M 0535–0546 (Figure 4), whose components have dynamical masses of 0.054 and 0.034  $M_{\odot}$  (Stassun et al. 2006)

To compare the masses and ages of FU Tau A and B to those of previously known young low-mass binaries, we have included the components of 2M J1101–7732, Oph 1622–2405, and USco CTIO 108 in Figure 5. Because the optical spectra of these systems and FU Tau have been directly compared (Figure 4; Luhman et al. 2007a; Béjar et al. 2008), their relative spectral types should be quite accurate. In addition, the spectral types and photometry have been converted to temperatures and luminosities with the same methods that we have applied to FU Tau. As shown in Figure 5, FU Tau A probably has a mass that is similar to those of the other three primaries while FU Tau B may be slightly less massive than Oph 1622–2405 B and USco CTIO 108 B. The most striking aspect of this comparison is that the luminosity ratio of FU Tau A and B ( $L_A/L_B \sim 80$ ) is much larger than the ratios in the other systems ( $L_A/L_B = 1.6\text{--}16$ ), further illustrating that one of the components of FU Tau (probably the primary) has an anomalous luminosity.

### 3.3. Spectral Energy Distributions

We selected FU Tau A as a candidate member of Taurus because it exhibits mid-IR colors that are indicative of a circumstellar disk. To demonstrate the presence of this mid-IR excess emission from FU Tau A and to determine whether its companion has a disk, we have constructed their SEDs using the photometry compiled in Table 1. SDSS and IRAC have provided photometry at multiple epochs for the FU Tau system; we adopt the average of the available measurements for a given SDSS band and we use the IRAC data from 2007 since the camera observed FU Tau in only two bands in the other epoch. In addition to the photometry, we include in the SED for FU Tau A the low-resolution IR spectrum obtained with SpeX, which has been flux-calibrated with the photometry from 2MASS. The resulting SEDs of FU Tau A and B are presented in Figure 6.

To determine if the SEDs contain excess emission at short or long wavelengths, we compare them to the SEDs of stellar photospheres. We construct an estimate of the photospheric SEDs of FU Tau A and B from data for the Taurus members KPNO 5 and KPNO 4, respectively, which have similar spectral types as FU Tau A and B, have negligible extinction, and lack mid-IR excess emission and significant accretion (Briceño et al. 2002; Muzerolle et al. 2005; Hartmann et al. 2005; Luhman et al. 2006). Optical measurements in the SDSS and  $I$  bands for the KPNO objects are taken from Finkbeiner et al. (2004) and Briceño et al. (2002). Because KPNO 4 has a very low signal-to-noise ratio at  $r$ , we compute the flux in this band by combining the  $i$  photometry for KPNO 4 with the typical value of  $r - i$  for M9 dwarfs (Kraus & Hillenbrand 2007). For KPNO 5, we include a low-resolution IR spectrum collected with SpeX (Muench et al. 2007). For the mid-IR portion of these photospheric SEDs, we adopt the average colors of disk-

less stars near the spectral types of FU Tau A and B (Luhman et al. 2008). The template for FU Tau A is reddened by  $A_V = 2$  according to the reddening laws from Rieke & Lebofsky (1985) and Flaherty et al. (2007). The photospheric SEDs are then normalized to the  $J$ - and  $K$ -band fluxes of FU Tau A and B, respectively. Relative to these SEDs, both FU Tau A and B exhibit significant excess emission at wavelengths longward of 4  $\mu\text{m}$ , as shown in Figure 6. The primary also has excess emission in the bluest optical and UV bands, which probably explains why its optical spectrum implies less extinction than the near-IR data (§ 3.1).

To classify the SEDs of FU Tau A and B according to the standard scheme for young stars (Lada 1987; Greene et al. 1994), we use the IR spectral slope that is defined as  $\alpha = d \log(\lambda F_{\lambda}) / d \log(\lambda)$  (Lada & Wilking 1984; Adams et al. 1987). The extinction-corrected slopes between 3.6 and 8  $\mu\text{m}$  for each object are given in Table 3. By applying the thresholds from Luhman et al. (2008) to these slopes, we classify the SEDs of FU Tau A and B as Class II.

### 3.4. Evidence of Membership in Taurus

The components of FU Tau clearly have ages of  $\sim 1$  Myr based on their H $\alpha$  emission, mid-IR excess emission, and gravity-sensitive spectral features. Given that they are projected against the center of Barnard 215, it is likely that they were born in this cloud, which is a part of the Taurus star-forming region. The SDSS images of Barnard 215 also show faint nebulosity centered on FU Tau, which supports its association with the cloud. The proper motion of FU Tau represents an additional constraint on its membership. Indeed, Jones & Herbig (1979) identified FU Tau has a likely member of Taurus through a measurement of its proper motion. We now perform a new analysis of the motion of FU Tau that makes use of the astrometric data that are currently available.

In Table 4, we list proper motion measurements for FU Tau A from the USNO-B1.0 catalog (Monet et al. 2003) and Ducourant et al. (2005). We also include our measurement of the proper motion, which is based on positions in the USNO-A2.0 catalog (Monet et al. 1998, epoch 1950.9), the Guide Star Catalog V2.3.2 (STScI & Osservatorio Astronomico di Torino 2006, epoch 1994.8), the 2MASS Point Source Catalog (Skrutskie et al. 2006, epoch 1997.9), and the Carlsberg Meridian Catalog Vol. 14 (CDS catalog I/304; epoch 2001.8). Our estimate is similar to the value from USNO-B1.0. We adopt our measurement of the proper motion in the following discussion.

What is the proper motion of a hypothetical member of Taurus at the position of FU Tau A? Because Taurus covers a large solid angle of sky, the proper motion for a given velocity vector varies across the association due to geometric projection effects. For this calculation, we adopt a mean Galactic velocity vector of  $(U, V, W) = (-16.5, -13.2, -11.0)$  km s $^{-1}$  (Bertout & Genova 2006) and a mean distance of 140 pc for Taurus (Wichmann et al. 1998; Loinard et al. 2005; Torres et al. 2007). At the position of FU Tau A, we predict that a star with the mean velocity vector of Taurus would have a proper motion of  $\mu_{\alpha^*} = +8.4$  (140 pc/d) mas yr $^{-1}$  and  $\mu_{\delta} =$

$-23.5$  (140 pc/ $d$ ) mas yr $^{-1}$ , where  $d$  is the distance in pc. The mean velocity vector is constrained to  $\pm 1$  km s $^{-1}$  in each component, which translates to an uncertainty of  $\sim 1$  mas yr $^{-1}$  in the predicted proper motion for a given distance. Hence, we find that our predicted values of  $\mu_{\alpha^*}$  and  $\mu_{\delta}$  for an “ideal” Taurus member are within  $0.3\sigma$  and  $1.7\sigma$  of the observed motion, respectively. The predicted motion is also within  $1.1\sigma$  and  $2.4\sigma$  of the USNO-B1.0  $\mu_{\alpha^*}$  and  $\mu_{\delta}$  motions, respectively. For comparison, in Table 4 we also include the predicted proper motions for hypothetical members of the Hyades and Pleiades open clusters at their respective mean distances, which are based on data from de Bruijne et al. (2001), Robichon et al. (1999), and Soderblom et al. (2005). Both groups are known to have members in the vicinity of Taurus. However, the motion of FU Tau A is completely inconsistent with the kinematic membership of either of these clusters. Based on this analysis, we conclude that the proper motion of FU Tau A is in good agreement with the average motion of the stellar population in Taurus. According to the astrometric measurements of FU Tau A and B in Table 2, the pair maintained the same relative positions to within  $\sim 0.1''$  across a period of three years, indicating that the secondary shares the same motion as the primary at a level of  $\sim 30$  mas yr $^{-1}$ .

It is useful to compare the motion of FU Tau A to that of FT Tau, which is the only other known young star that is projected against the Barnard 215 cloud (Figure 1). We have measured the proper motion of FT Tau using the same catalogs that were employed for FU Tau A, arriving at values of  $\mu_{\alpha^*} = +6.3 \pm 3.3$  mas yr $^{-1}$  and  $\mu_{\delta} = -15.3 \pm 3.3$  mas yr $^{-1}$ . The motions of the two objects agree to within  $1.1 \pm 4.9$  and  $2.2 \pm 4.7$  mas yr $^{-1}$  in right ascension and declination, respectively, which translates into tangential velocities at 140 pc that agree to within  $0.7 \pm 3.3$  and  $1.5 \pm 3.1$  km s $^{-1}$ . These relative motions indicate that FU Tau A has remained within a projected distance of 1.7 pc ( $0.7^\circ$ ) from FT Tau during its lifetime ( $\tau \lesssim 1$  Myr, Figure 5). The agreement in their velocities and the presence of nebulosity centered on each source strongly suggests that they are associated with the Barnard 215 cloud and were not born elsewhere.

Finally, we have searched for evidence of additional young stars near Barnard 215. Aside from FU Tau and FT Tau, the only other candidate young star that has been previously identified near the cloud is GT Tau (Jones & Herbig 1979). Through an analysis similar to that performed for FU Tau and FT Tau, we find that the proper motion of GT Tau is inconsistent with membership in Taurus. Previous surveys for young stars in the vicinity of Barnard 215 have been conducted at optical wavelengths, and thus could have missed stars that are embedded within the cloud. The mid-IR images from *Spitzer* that were used to uncover FU Tau easily penetrate the extinction of Barnard 215, and they do not reveal any additional disk-bearing stars. We cannot rule out the presence of diskless young stars within the cloud given that they would be indistinguishable from field stars in *Spitzer* data. However, it is unlikely that an embedded population within the cloud would consist of only diskless stars.

### 3.5. Evidence of Binarity

We have presented strong evidence indicating that FU Tau A and B are members of the Taurus star-forming region. We have also shown that they have similar proper motions, but the accuracy of these measurements is insufficient to distinguish between a binary system and a pair of unrelated members of Taurus that are seen in projection near each other. Therefore, as in most studies of visual pairs in star-forming regions, we rely on a statistical analysis to assess whether FU Tau A and B are likely to comprise a binary system. Because of the low stellar density in Taurus, it is unlikely that a given member of the region will appear close to another member on the sky, unless they are in a binary system. This probability is particularly low for FU Tau, which resides in one of the most isolated dark clouds in Taurus. As shown in Figure 2, only one young star has been found within a radius of  $0.5^\circ$  surrounding FU Tau. We can roughly quantify the probability that FU Tau is a pair of unrelated low-mass Taurus members. Among the 51 known members of Taurus that have spectral types later than M6, the median distance to the nearest  $>M6$  neighbor is  $22.3'$ . For our probability calculation, we adopt a population of 51 objects that are randomly distributed across an area of  $32.5$  deg $^2$ , which exhibits a median nearest neighbor distance that is similar to the observed value. The probability of finding a pair of objects in this population with a projected separation of  $a \leq 6''$  is  $3 \times 10^{-4}$ . Therefore, it is likely that FU Tau A and B comprise a binary system.

## 4. DISCUSSION

With component masses of  $\sim 0.05$  and  $\sim 0.015 M_\odot$  and a projected separation of 800 AU, FU Tau joins the growing sample of wide low-mass binaries that have been discovered in recent years (§ 1). These systems have provided valuable constraints on theories of the formation of brown dwarfs (Luhman 2004a). Unlike the previously known binaries – or free-floating brown dwarfs, for that matter – FU Tau A and B are the first spectroscopically-confirmed brown dwarfs discovered forming in isolation<sup>8</sup>. The unique formation environment of FU Tau represents a new test of theoretical models for the origin of brown dwarfs.

As reviewed in § 1, dynamical models typically create brown dwarfs through ejection from protostellar clusters (Reipurth & Clarke 2001; Bate et al. 2002) or fragmentation of disks around stars and subsequent stripping of the substellar companion through encounters with other stars (Goodwin & Whitworth 2007; Stamatellos et al. 2007). Because both mechanisms require the presence of stellar clusters, they cannot account for the existence of brown dwarfs like FU Tau A and B that are forming in isolation. Although the disk fragmentation models produce brown dwarfs as companions to stars, and those stars can be isolated, this scenario is not plausible for FU Tau because the mass and separation of the secondary are much larger than the (limited) mea-

<sup>8</sup> FU Tau may comprise a more evolved version of L1014-IRS, which is an isolated low-mass protostar (Young et al. 2004; Bourke et al. 2005; Huard et al. 2006). Its current and ultimate masses are uncertain because it is extremely young and highly embedded.

measurements of masses and radii for brown dwarf disks ( $r \sim 30$  AU,  $M \sim 1 M_{\text{Jup}}$ ; Klein et al. 2003; Scholz et al. 2006; Luhman et al. 2007c).

The discovery of FU Tau demonstrates that brown dwarfs can arise in isolation without the involvement of dynamical interactions among stars. It is likely that the same process that made it possible for substellar objects to form in Barnard 215 also occurs in clusters as well. Thus, it is unnecessary to invoke additional mechanisms like ejection for creating brown dwarfs unless observations indicate their presence. Dynamical interactions in young clusters probably do affect the formation of brown dwarfs, just as they affect the formation of stars, but there is no evidence to date that they represent a second dominant mechanism that enables the birth of brown dwarfs (Luhman et al. 2007b).

We thank Lee Hartmann for helpful comments on the manuscript. K. L. was supported by grant AST-0544588 from the National Science Foundation (NSF) and E. M. was supported by a Clay Postdoctoral Fellowship from the Smithsonian Astrophysical Observatory. This publication makes use of data products from 2MASS, which is a joint project of the University of Massachusetts and the Infrared Processing and Analysis Center/California Institute of Technology, funded by NASA and the NSF. The Guide Star Catalogue-II is a joint project of the Space Telescope Science Institute and the Osservatorio Astronomico di Torino. Space Telescope Science Institute is operated by the Association of Universities for Research in Astronomy, for NASA under contract NAS5-26555. The participation of the Osservatorio As-

tronomico di Torino is supported by the Italian Council for Research in Astronomy. Additional support is provided by European Southern Observatory, Space Telescope European Coordinating Facility, the International GEMINI project and the European Space Agency Astrophysics Division. This research used the facilities of the Canadian Astronomy Data Centre operated by the National Research Council of Canada with the support of the Canadian Space Agency. Funding for SDSS has been provided by the Alfred P. Sloan Foundation, the Participating Institutions, the NSF, the U.S. Department of Energy, NASA, the Japanese Monbukagakusho, the Max Planck Society, and the Higher Education Funding Council for England. The SDSS is managed by the Astrophysical Research Consortium for the Participating Institutions. The Participating Institutions are the American Museum of Natural History, Astrophysical Institute Potsdam, University of Basel, University of Cambridge, Case Western Reserve University, The University of Chicago, Drexel University, Fermilab, the Institute for Advanced Study, the Japan Participation Group, The Johns Hopkins University, the Joint Institute for Nuclear Astrophysics, the Kavli Institute for Particle Astrophysics and Cosmology, the Korean Scientist Group, the Chinese Academy of Sciences, Los Alamos National Laboratory, the Max-Planck-Institute for Astronomy, the Max-Planck-Institute for Astrophysics, New Mexico State University, Ohio State University, University of Pittsburgh, University of Portsmouth, Princeton University, the United States Naval Observatory, and the University of Washington.

## REFERENCES

- Adams, F. C., Lada, C. J., & Shu, F. H. 1987, *ApJ*, 571, 378  
 Adelman-McCarthy, J., et al. 2008, *ApJS*, 175, 297  
 Allers, K. N. 2006, PhD thesis, University of Texas, Austin  
 Artigau, E., Lafrenière, D., Doyon, R., Albert, L., Nadeau, D., & Robert, J. 2007, *ApJ*, 659, L49  
 Baraffe, I., Chabrier, G., Allard, F., & Hauschildt, P. H. 1998, *A&A*, 337, 403  
 Barnard, E. E., Frost, E. B., & Calvert, M. R. 1927, *A Photographic Atlas of Selected Regions of the Milky Way* (Washington: Carnegie Inst.)  
 Bate, M. R., & Bonnell, I. A. 2005, *MNRAS*, 356, 1201  
 Bate, M. R., Bonnell, I. A., & Bromm, V. 2002, *MNRAS*, 332, L65  
 Béjar, V. J. S., Zapatero Osorio, M. R., Pérez-Garrido, A., Álvarez, C., Martín, E. L., Rebolo, R., Villó-Pérez, I., & Díaz-Sánchez, A. 2008, *ApJ*, 673, L185  
 Bertout, C., & Genova, F. 2006, *A&A*, 460, 499  
 Billères, M., Delfosse, X., Beuzit, J.-L., Forveille, T., Marchal, L., & Martín, E. L. 2005, *A&A*, 440, L55  
 Boss, A. 2001, *ApJ*, 551, L167  
 Bourke T. L., et al. 2005, *ApJ*, 633, L129  
 Briceño, C., Luhman, K. L., Hartmann, L., Stauffer, J. R., & Kirkpatrick, J. D. 2002, *ApJ*, 580, 317  
 de Bruijne, J. H. J., Hoogerwerf, R., & de Zeeuw, P. T. 2001, *A&A*, 367, 111  
 Burgasser, A. J., Reid, I. N., Siegler, N., Close, L., Allen, P., Lowrance, P., Gizis, J. 2007, *Protostars and Planets V*, B. Reipurth, D. Jewitt, and K. Keil (eds.), University of Arizona Press, Tucson, 427  
 Caballero, J. A. 2007, *A&A*, 462, L61  
 Caballero, J. A., Martín, E. L., Dobbie, P. D., & Barrado y Navascués, D. 2006, *A&A*, 460, 635  
 Casali, M., et al. 2007, *A&A*, 467, 777  
 Chabrier, G., Baraffe, I., Allard, F., & Hauschildt, P. 2000, *ApJ*, 542, L119  
 Chauvin, G., et al. 2004, *A&A*, 425, L29  
 Close, L. M., et al. 2007, *ApJ*, 660, 1492  
 Cushing, M. C., Vacca, W. D., & Rayner, J. T. 2004, *PASP*, 116, 362  
 Dahn, C. C., et al. 2002, *AJ*, 124, 1170  
 Delgado-Donate, E. J., Clarke, C. J., & Bate, M. R. 2003, *MNRAS*, 342, 926  
 Dobashi, K., Uehara, H., Kandori, R., Sakurai, T., Kaiden, M., Umemoto, T., & Sato, F. 2005, *PASJ*, 57, 1  
 Ducourant, C., Teixeira, R., Périé, J. P., Lecampion, J. F., Guibert, J., & Sartori, M. J. 2005, *A&A*, 438, 769  
 Dye, S., et al. 2006, *MNRAS*, 372, 1227  
 Fazio, G. G., et al. 2004, *ApJS*, 154, 10  
 Finkbeiner, D. P., et al. 2004, *AJ*, 128, 2577  
 Flaherty, K. M., Pipher, J. L., Megeath, S. T., Winston, E. M., Gutermuth, R. A., Muzerolle, J., Allen, L. E., & Fazio, G. G. 2007, *ApJ*, 663, 1069  
 Fukugita, M., Ichikawa, T., Gunn, J. E., Doi, M., Shimasaku, K., & Schneider, D. P. 1996, *AJ*, 111, 1748  
 Gizis, J. E., Reid, I. N., & Hawley, S. L. 2002, *AJ*, 123, 3356  
 Goodwin, S. P., & Whitworth, A. 2007, *A&A*, 466, 943  
 Gorlova, N. I., Meyer, M. R., Rieke, G. H., & Liebert, J. 2003, *ApJ*, 593, 1074  
 Greene, T. P., Wilking, B. A., André, P., Young, E. T., & Lada, C. J. 1994, *ApJ*, 434, 614  
 Guieu, S., Dougados, C., Monin, J.-L., Magnier, E., & Martín, E. L. 2006, *A&A*, 446, 485  
 Hambly, R. C., et al. 2008, *MNRAS*, 384, 637  
 Haro, G., Iriarte, B., & Chavira, E. 1953, *Bol. Obs. Tonantzintla y Tacubaya*, 8, 3  
 Hartmann, L., Megeath, S. T., Allen, L., Luhman, K., Calvet, N., D'Alessio, P., Franco-Hernandez, R., & Fazio, G. 2005, *ApJ*, 629, 881

- Hewett, P. C., Warren S. J., Leggett S. K., & Hodgkin S. L., 2006, *MNRAS*, 367, 545
- Huard, T. L., et al. 2006, *ApJ*, 640, 391
- Jayawardhana, R., & Ivanov, V. D. 2006, *Science*, 313, 1279
- Jones, B. F., & Herbig, G. H. 1979, *AJ*, 84, 1872
- Kenyon, S. J., Gómez, M., & Whitney, B. A. 2008, *Handbook of Star Forming Regions*, ASP Conference Series, in press
- Kholopov, P. N., et al. 1998, *Combined General Catalogue of Variable Stars*
- Klein, R., Apai, D., Pascucci, I., Henning, Th., Waters, L. B. F. M. 2003, *ApJ*, 593, L57
- Kraus, A. L., & Hillenbrand, L. A. 2007, *AJ*, 134, 2340
- Lada, C. J. 1987, in *IAU Symp. 115, Star Forming Regions*, ed. M. Peimbert & J. Jugaku (Dordrecht: Reidel), 1
- Lada, C. J., & Wilking, B. A. 1984, *ApJ*, 287, 610
- Landolt, A. U. 1992, *AJ*, 104, 340
- Lawrence, A., et al. 2007, *MNRAS*, 379, 1599
- Lee, C. W., & Myers, P. C. 1999, *ApJS*, 123, 233
- Loinard, L., Mioduszewski, A. J., Rodríguez, L. F., González, R. A., Rodríguez, M. I., & Torres, R. M. 2005, *ApJ*, 619, L179
- Lucas, P. W., Roche, P. F., Allard, F., & Hauschildt, P. H. 2001, *MNRAS*, 326, 695
- Luhman, K. L. 1999, *ApJ*, 525, 466
- Luhman, K. L. 2004a, *ApJ*, 614, 398
- Luhman, K. L. 2004b, *ApJ*, 617, 1216
- Luhman, K. L. 2007, *ApJS*, 173, 104
- Luhman, K. L., Allers, K. N., Jaffe, D. T., Cushing, M. C., Williams, K. A., Slesnick, C. L., & Vacca, W. D. 2007a, *ApJ*, 659, 1629
- Luhman, K. L., Joergens, V., Lada, C., Muzerolle, J., Pascucci, I., & White, R. 2007b, *Protostars and Planets V*, B. Reipurth, D. Jewitt, and K. Keil (eds.), University of Arizona Press, Tucson, 443
- Luhman, K. L., Rieke, G. H., Lada, C. J., & Lada, E. A. 1998, *ApJ*, 508, 347
- Luhman, K. L., Stauffer, J. R., Muench, A. A., Rieke, G. H., Lada, E. A., Bouvier, J., & Lada, C. J. 2003, *ApJ*, 593, 1093
- Luhman, K. L., Whitney, B. A., Meade, M. R., Babler, B. L., Indebetouw, R., Bracker, S., & Churchwell, E. B. 2006, *ApJ*, 647, 1180
- Luhman, K. L., et al. 2007c, *ApJ*, 666, 1219
- Luhman, K. L., et al. 2008, *ApJ*, 675, 1375
- Lynds, B. T. 1962, *ApJS*, 7, 1
- Marengo, M., Megeath, S. T., Fazio, G. G., Stapelfeldt, K. R., Werner, M. W., Backman, D. E. 2006, *ApJ*, 647, 1437
- Martín, E. L., Rebolo, R., & Zapatero Osorio, M. R. 1996, *ApJ*, 469, 706
- McGovern, M. R., Kirkpatrick, J. D., McLean, I. S., Burgasser, A. J., Prato, L., & Lowrance, P. J. 2004, *ApJ*, 600, 1020
- Monet, D. G., et al. 1998, *USNO-A2.0 Catalog (Flagstaff: USNO)*
- Monet, D. G., et al. 2003, *AJ*, 125, 984 (USNO-B1.0)
- Muench, A. A., Lada, C. J., Luhman, K. L., Muzerolle, J., & Young, E. 2007, *AJ*, 134, 411
- Muzerolle, J., Luhman, K. L., Briceño, C., Hartmann, L., & Calvet, N. 2005, *ApJ*, 625, 906
- Nercessian, E., Castets, A., Benayoun, J. J., & Cernicharo, J. 1988, *A&A*, 189, 207
- Padmanabhan, N., et al. 2008, *ApJ*, 674, 1217
- Rayner, J. T., et al. 2003, *PASP*, 115, 362
- Reipurth, B. & Clarke, C. 2001, *AJ*, 122, 432
- Rieke, G. H., & Lebofsky, M. J. 1985, *ApJ*, 288, 618
- Rieke, G. H. et al. 2004, *ApJS*, 154, 25
- Robichon, N., Arenou, F., Mermilliod, J.-C., & Turon, C. 1999, *A&A*, 345, 471
- Scholz, A., Jayawardhana, R., & Wood, K. 2006, *ApJ*, 645, 1498
- Skrutskie, M., et al. 2006, *AJ*, 131, 1163
- Soderblom, D. R., Nelan, E., Benedict, G. F., McArthur, B., Ramirez, I., Spiesman, W., & Jones, B. F. 2005, *AJ*, 129, 1616
- Space Telescope Science Institute and Osservatorio Astronomico di Torino, 2006, *The Guide Star Catalogue, Version 2.3.2*, CDS catalogue I/305
- Stamatellos, D., Hubber, D. A., & Whitworth, A. P. 2007, *MNRAS*, 382, L30
- Stassun, K. G., Mathieu, R. D., & Valenti, J. A. 2006, *Nature*, 440, 311
- Torres, R. M., Loinard, L., Mioduszewski, A. J., & Rodríguez, L. F. 2007, *ApJ*, 671, 1813
- Umbreit, S., Burkert, A., Henning, T., Mikkola, S., & Spurzem, R. 2005, *ApJ*, 623, 940
- Vacca, W. D., Cushing, M. C., & Rayner J. T., 2003, *PASP*, 115, 389
- Warren, S. J., et al. 2007, *MNRAS*, 375, 213
- Werner, M. W., et al. 2004, *ApJS*, 154, 1
- White, R. J., Ghez, A. M., Reid, I. N., & Schultz, G. 1999, *ApJ*, 520, 811
- Wichmann, R., Bastian, U., Krautter, J., Jankovics, I., & Ruciński, S. M. 1998, *MNRAS*, 301, L39
- York, D. G., et al. 2000, *AJ*, 120, 1579
- Young, C. H., et al. 2004, *ApJS*, 154, 396



TABLE 1  
PHOTOMETRY FOR FU TAU A AND B

Band	A	B	Date
<i>u</i>	20.14±0.06	...	2002 Dec 6
<i>u</i>	19.43±0.05	...	2002 Dec 29
<i>g</i>	19.13±0.05	...	2002 Dec 6
<i>g</i>	18.69±0.05	...	2002 Dec 29
<i>r</i>	17.13±0.05	22.6±0.3	2002 Dec 29
<i>r</i>	16.86±0.05	22.8±0.3	2002 Dec 29
<i>i</i>	14.86±0.05	20.45±0.06	2002 Dec 6
<i>i</i>	14.75±0.05	20.62±0.06	2002 Dec 29
<i>z</i>	13.12±0.05	18.23±0.05	2002 Dec 6
<i>z</i>	13.05±0.05	18.11±0.05	2002 Dec 29
<i>I</i>	13.58±0.04	18.80±0.05	2002 Dec 29
<i>J</i>	10.78±0.02	...	1997 Nov 29
<i>H</i>	9.95±0.03	...	1997 Nov 29
<i>K<sub>s</sub></i>	9.32±0.02	...	1997 Nov 29
<i>K</i>	saturated	13.33±0.02	2005 Dec 31
[3.6]	out	out	2005 Feb 23
[3.6]	8.34±0.02	12.54±0.1	2007 Mar 3
[4.5]	7.68±0.02	11.90±0.1	2005 Feb 23
[4.5]	7.87±0.02	11.93±0.1	2007 Mar 3
[5.8]	out	out	2005 Feb 23
[5.8]	7.33±0.03	11.46±0.1	2007 Mar 3
[8.0]	6.45±0.03	10.77±0.1	2005 Feb 23
[8.0]	6.72±0.03	10.87±0.1	2007 Mar 3
[24]	4.56±0.04	...	2007 Feb 2

NOTE. — Data are from SDSS (*ugriz*), CFHT (*I*), 2MASS (*JHK<sub>s</sub>*), UKIDSS (*K*), and *Spitzer* (3.6–24  $\mu$ m).

TABLE 2  
ASTROMETRY FOR FU TAU A AND B

Source	Separation (arcsec)	PA (deg)	Date
CFHT	5.61±0.1	123.0±1	2002 Dec 29
SDSS	5.67±0.1	123.4±1	2002 Dec 6, 29
UKIDSS	5.72±0.1	123.2±1	2005 Dec 31

TABLE 3  
PROPERTIES OF FU TAU A AND B

FU Tau	Spectral Type	$T_{\text{eff}}^{\text{a}}$ (K)	$A_V$	$L_{\text{bol}}$ ( $L_{\odot}$ )	Membership Evidence <sup>b</sup>	$W_{\lambda}(\text{H}\alpha)$ ( $\text{\AA}$ )	$\alpha(3.6\text{--}8\ \mu\text{m})$
A	M7.25±0.25	2838	2	0.19	NaK, H <sub>2</sub> O, ex, e, $\mu$	93±7	−1.02
B	M9.25±0.25	2375	< 1	0.0039	NaK, ex, e	~70	−0.92

<sup>a</sup> Temperature scale from Luhman et al. (2003).

<sup>b</sup> Membership in Taurus is indicated by strong emission lines (“e”), Na I and K I strengths intermediate between those of dwarfs and giants (“NaK”), the shape of the gravity-sensitive steam bands (“H<sub>2</sub>O”), IR excess emission (“ex”), or a proper motion (“ $\mu$ ”) that is similar to that of the known members of the star-forming region.

TABLE 4  
OBSERVED AND PREDICTED PROPER MOTIONS OF FU TAU A

	Observed			Predicted		
	USNO-B1.0 <sup>a</sup>	Duc05 <sup>b</sup>	this work	Taurus	Hyades	Pleiades
$\mu_{\alpha^*}$	+6 ± 2	+14 ± 7	+7.2 ± 3.6	+8.4	+109.3	+14.5
$\mu_{\delta}$	−18 ± 2	−26 ± 7	−17.5 ± 3.4	−23.5	−52.9	−47.2

NOTE. — Units are mas yr<sup>−1</sup>.

<sup>a</sup> Monet et al. (2003).

<sup>b</sup> Ducourant et al. (2005).



FIG. 1.— Optical image of the Barnard 215 dark cloud obtained by SDSS (Finkbeiner et al. 2004). FU Tau A and B are at the center of the image. The only other known member of Taurus within this field is FT Tau, which is the star surrounded by extended emission in the lower middle of the image. The red, green, and blue image planes correspond to the  $i$ ,  $r$ , and  $g$  filters, respectively. The size of the image is  $0.5^\circ \times 0.5^\circ$ . North is up and East is left

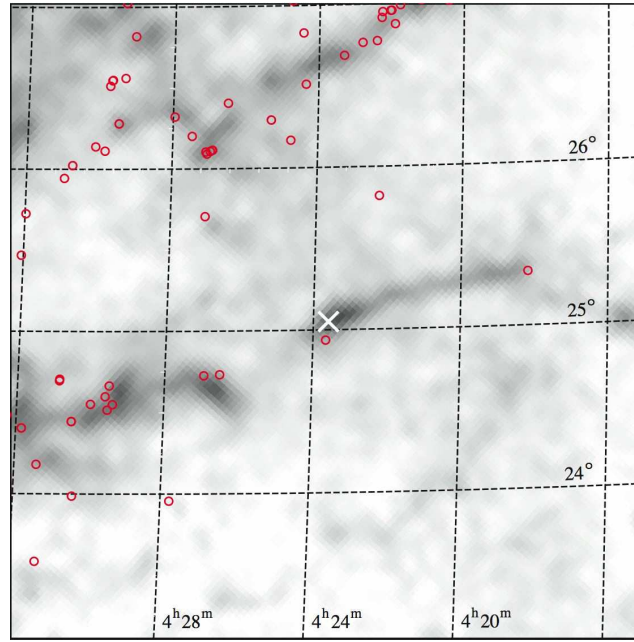


FIG. 2.— Extinction map from Dobashi et al. (2005) for a  $2^\circ \times 2^\circ$  field in the Taurus star-forming region centered on FU Tau A and B (*cross*). The positions of known members of Taurus are indicated (*circles*).

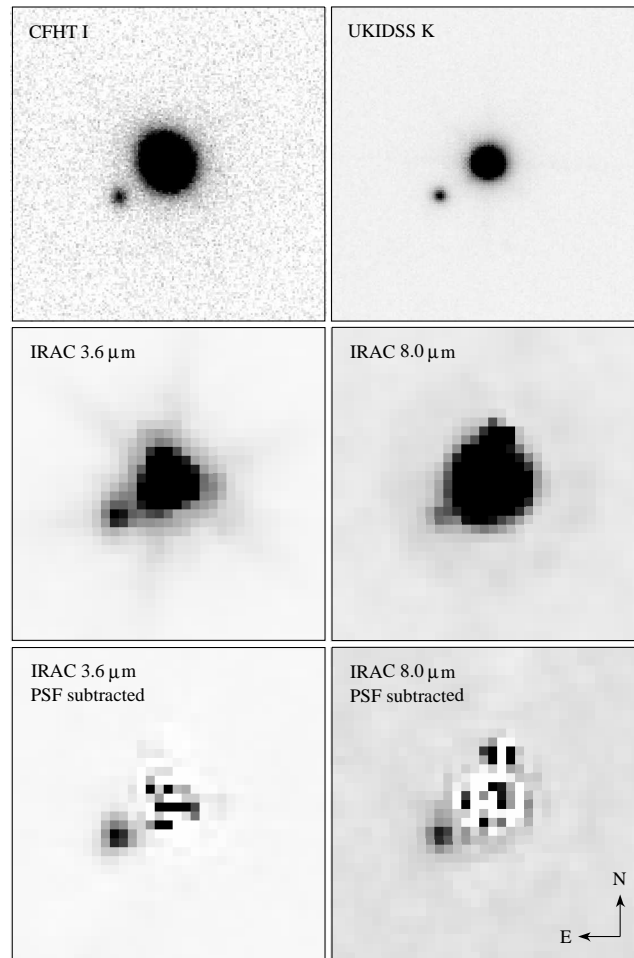


FIG. 3.— Optical and IR images of FU Tau A and B. The size of each image is  $30'' \times 30''$ .

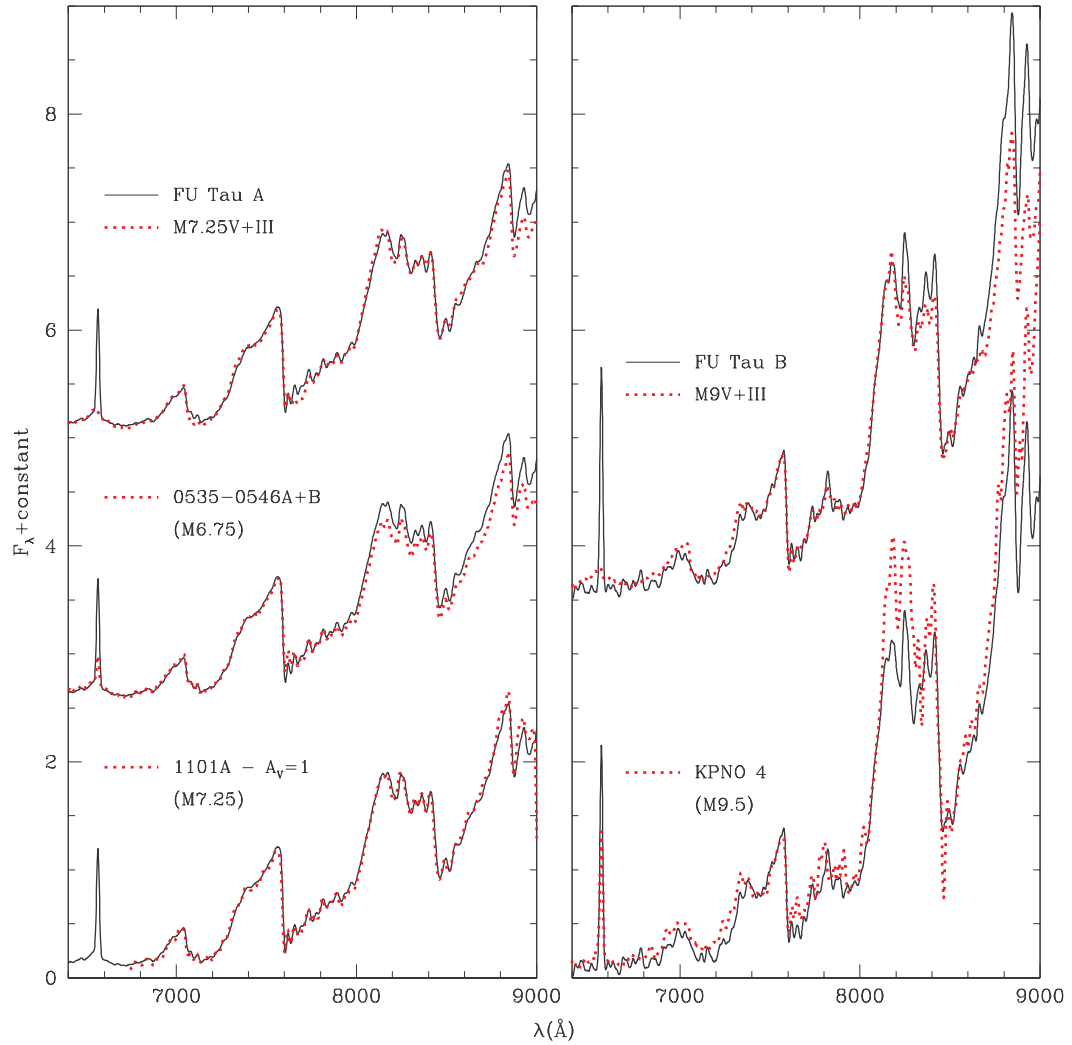


FIG. 4.— Optical spectra of FU Tau A and B (*solid lines*) compared to data for pre-main-sequence and field standards (*dotted lines*). *Left:* After comparing FU Tau A to averages of standard dwarfs and giants, we find that M7.25 provides the best match. Its spectrum is slightly later than the composite spectrum of the eclipsing binary 2M 0535–0546 ( $0.034$  and  $0.054 M_{\odot}$ ; Stassun et al. 2006) and is very similar to the primary in the young binary 2M 1101–7732 (M7.25; Luhman 2004a). *Right:* FU Tau B is slightly later than an average of M9 dwarfs and giants and is earlier than the Taurus member KPNO 4 (M9.5; Briceño et al. 2002), leading to a classification of M9.25. The data are displayed at a resolution of  $18 \text{ \AA}$  and are normalized at  $7500 \text{ \AA}$ .

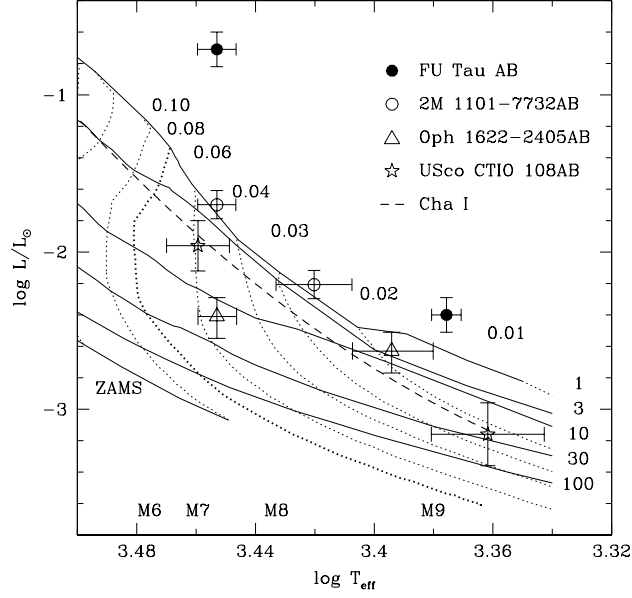


FIG. 5.— H-R diagram for the components of the binaries FU Tau (*filled circles*, Table 3), 2M J1101-7732 (*open circles*, Luhman 2004a), Oph 1622-2405 (*triangles*, Luhman et al. 2007a), and USco CTIO 108 (*stars*, Béjar et al. 2008). These data are shown with a fit to the empirical cluster sequence for Chamaeleon I (*dashed line*; Luhman 2007) and the theoretical evolutionary models of Baraffe et al. (1998) ( $0.1 < M/M_{\odot} \leq 1$ ) and Chabrier et al. (2000) ( $M/M_{\odot} \leq 0.1$ ), where the mass tracks (*dotted lines*) and isochrones (*solid lines*) are labeled in units of  $M_{\odot}$  and Myr, respectively.

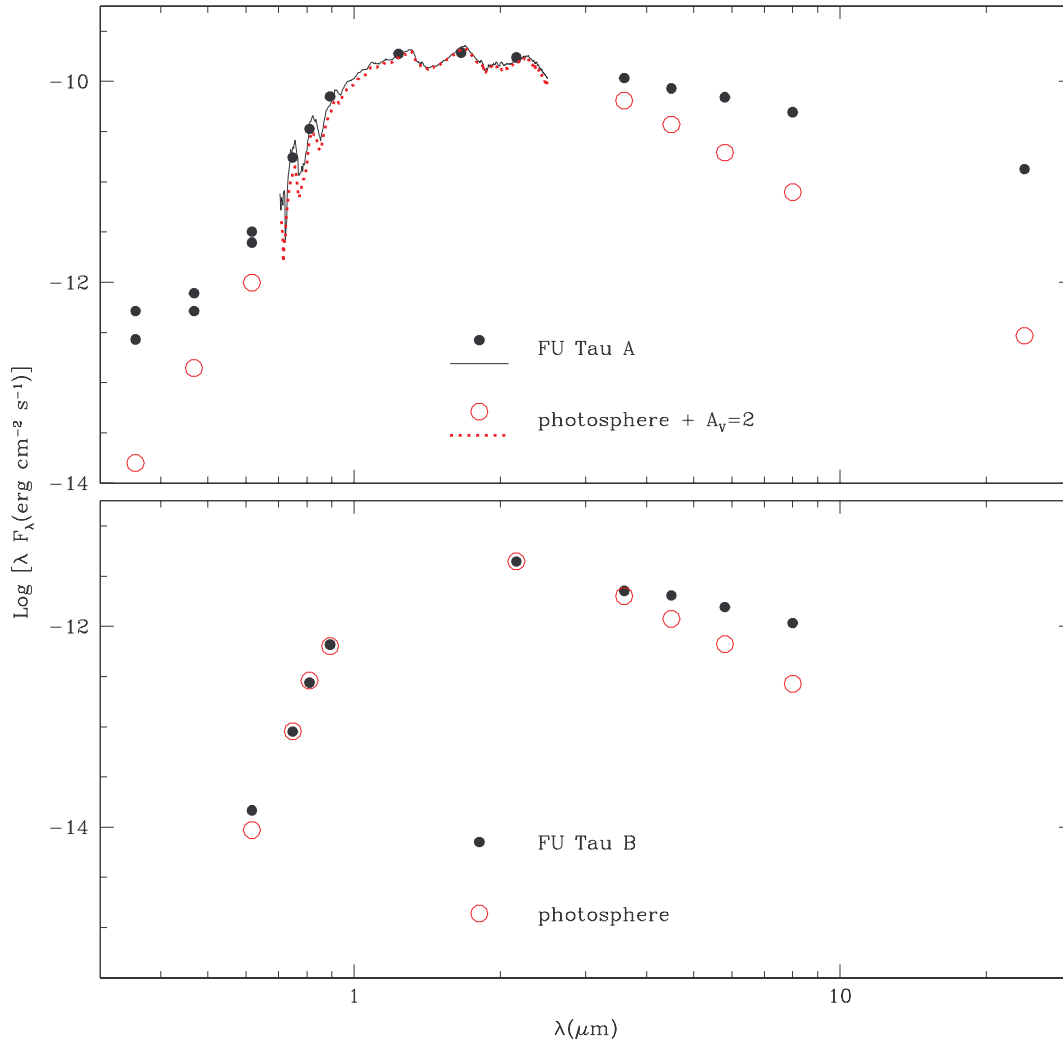


FIG. 6.— SEDs for FU Tau A and B compared to the SEDs of stellar photospheres with the same spectral types. The two epochs of photometry at  $u$ ,  $g$ , and  $r$  ( $0.35$ ,  $0.47$ ,  $0.62 \mu\text{m}$ ) for the primary are plotted separately while other data at multiple epochs are averaged. The photospheric SEDs have been scaled to the photometry at  $J$  and  $K$  for the primary and secondary, respectively.